International Journal of Mass Spectrometry 189 (1999) 79–92

Organic substances in cometary grains: comparison of secondary ion mass spectral data and californium-252 plasma desorption data from reference compounds

K. Varmuza[a,]*, W. Werther[b], F.R. Krueger[c], J. Kissel[d], E.R. Schmid[b]

[a]*Laboratory for Chemometrics, Institute of Food Chemistry and Food Technology, Vienna University of Technology, Getreidemarkt 9/160, A-1060 Vienna, Austria*
[b]*Institute of Analytical Chemistry, University of Vienna, Währinger Strasse 38, A-1090 Vienna, Austria*
[c]*Ingenieurbureau Dr. Krueger, Messeler Strasse 24, D-64291 Darmstadt, Germany*
[d]*Max-Planck-Institute for Extraterrestrial Physics, Giessenbachstrasse, D-85748 Garching, Germany*

Received 18 March 1999; accepted 12 April 1999

Abstract

Secondary ion mass spectra (SIMS) and ^{252}Cf plasma desorption ionization mass spectra (PDMS) of two carboxylic acids and two purine nucleobases have been compared. Results demonstrate that the positive ion mass spectra as well as the negative ion mass spectra are very similar in SIMS and PDMS. The principal characteristics are formation of quasimolecular ions $(M + H)^+$ or $(M-H)^-$ and loss of small molecules producing nonradical fragment ions; fumaric acid exhibits a remarkable formation of radical cations and anions. A set of simplified rules has been formulated for typical ion production processes involved in these techniques. This work contributes to the development of methods for data interpretation applicable to in situ analyses of cometary grains during the ROSETTA space mission of European Space Agency to the comet 46p/Wirtanen. (Int J Mass Spectrom 189 (1999) 79–92) © 1999 Elsevier Science B.V.

Keywords: SIMS; PDMS; Fragmentation processes; Cometary dust; ROSETTA; COSIMA

1. Introduction

Ionization methods based on the bombardment by particles play an increasing role in the analysis of surfaces, and of polar or less volatile refractory substances. Fast atom bombardment (FAB), secondary ion mass spectrometry (SIMS) and californium-252 plasma desorption mass spectrometry (PDMS) have been applied to a variety of compound classes [1]. Most of them are natural and artificial polymers, and their monomer building blocks. The spacecraft ROSETTA [2] of the European Space Agency (ESA) will carry a time-of-flight (TOF) SIMS instrument to the comet 46p/Wirtanen [3]. Within the project COSIMA (cometary secondary ion mass analyzer) it is planned to analyze in situ the organic and inorganic components of collected cometary grains [4]. Empirical information about the organic constituents [5] of cometary dust is solely based on measurements of ions produced by the high-speed impact of cometary dust particles on metal targets. Three such TOF mass

---

* Corresponding author. E-mail: kvarmuza@email.tuwien.ac.at

1387-3806/99/$20.00
PII S1387-3806(99)00069-X

spectrometers did encounter comet p/Halley in 1986, one of them (PIA) on board the European spacecraft GIOTTO [6] and two others (PUMA) on board the Soviet spacecrafts VEGA 1 and 2 [7]. The intimate mixture—presumably on a 10 nm scale [8–10]—of organic and inorganic material in cometary grains is considered to have been involved essentially in the development of self-reproducing molecules on earth, namely from precursors in the cometary grains in space [11].

In order to best use the limited resources onboard a spacecraft and with regard to the limited amount of data that can be sent back to earth, a considerable part of data interpretation will have to be performed automatically onboard. An efficient way for data reduction is based on the application of chemometric methods, and also requires a reasonable understanding of the ionization and fragmentation processes taking place. However, only little systematic knowledge is available about relationships between SIMS data and chemical structures that could be utilized for automatic data evaluation. In this work a few selected reference compounds have been measured with both a SIMS and a PDMS instrument in positive and negative ion modes. The selection was due to the presumable presence of substance classes (like nucleobases) or absence (dicarboxylic acids) in cometary dust. The resulting mass spectra have been compared with the aim of establishing basic rules that are typical for the ionization and fragmentation processes involved. These rules will be considered in a later phase of the COSIMA project for the definition of appropriate numerical spectral features that can be related to structural properties by applying chemometric methods [12,13].

2. Experimental

For the COSIMA investigations a TOF-SIMS instrument with an indium primary ion source will be used. For the present work a SIMS and a PDMS instrument were applied; both use a TOF mass analyzer and single ion counting.

2.1. SIMS instrument

A CAMECA TOF-SIMS IV instrument from ION-TOF GmbH (Münster, Germany) has been used with a gallium liquid metal source. The primary ion beam pulses, each containing some hundred ions, have a length of less than 1 ns (at best) and a spatial width of less than 1 μm. For our applications the spatial width has been broadened to about 10 μm to simulate the performance of the instrument onboard the spacecraft. The TOF-SIMS IV analyzer is equipped with a reflector and allows a maximum mass resolution of about 10 000. For this work a resolution $m/\Delta m$ of 3000 at 50% peak height has been chosen to be able to discriminate inorganic ions (for instance, from Mg, Ca, Fe silicates) from the organic ions of identical integer mass. The repetition frequency used was between 1 and 10 kHz. Each secondary ion is registered individually by its arrival time at the detector. Sum spectra are calculated automatically from that data.

Once a parent secondary ion is produced by desorption from the bulk surface because of the primary ion action, it may decay unimolecularly during the flight. For decay times below about 3 ns the daughter ion is observed at the detector. Decays between about 3 and 300 ns occur during secondary ion acceleration resulting in a line broadening. If the parent ion lifetime is between 300 ns and about 10 μs the produced daughter ion is reflected to the detector but the flight time cannot be correlated neither to the mass of the parent nor to the mass of the fragment ion.

2.2. PDMS instrument

The PDMS instrument used is a BIO-ION 20 from Bio-Ion Nordic AB (Uppsala, Sweden) with a 10 μC ^{252}Cf source, a flight tube of 141 mm in length, and no reflector. An acceleration potential of 15 kV was applied to the target relative to the grid in positive mode and -13 kV in negative mode. Typically, the ions produced by 1.6×10^6 shots (fission events) were accumulated in 2048 time channels (each 1 ns wide) corresponding to the mass range of 1–450 in positive mode and 1–380 in negative mode; mass

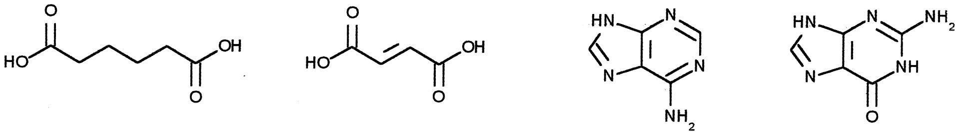

adipic acid $C_6H_{10}O_4$ mw 146

fumaric acid $C_4H_4O_4$ mw 116

adenine $C_5H_5N_5$ mw 135

guanine $C_5H_5N_5O$ mw 151

Fig. 1. Investigated compounds.

resolution $m/\Delta m$ was 80 at 50% peak height. The instrument is sensitive to ions produced within approximately 10 ns after desorption; ion decays within 10–300 ns lead to line broadening; for slower decays the daughter ion is observed at the flight time (mass) of the parent ion [14].

The fission particles impact randomly on an area of several tens of square millimeters and ions are produced around some 100 nm in diameter of the impact site. Thus, in PDMS nearly any impact excites a fresh zone of the sample whereas in SIMS the focused primary ion beam alters the material in the surface spot during the analysis.

2.3. Sample preparation

Samples have been prepared by either the electrospray technique, or, if not possible, by spin drying. Because of the fact that the mass spectra obtained depend upon the solvent used (especially with protic solvents) the same solvent has been used for SIMS and for PDMS. Nevertheless, the actual preparation may be a reason for differences between results from SIMS and PDMS because PDMS is a surface averaging method and SIMS acts on small spots.

2.4. Data evaluation

The new software PLUTO [15,16] has been developed for processing of PDMS raw data (number of ions per time channel). Automatic procedures and interactive tools were implemented for baseline correction, peak detection, background [17] subtraction, mass calibration, and deconvolution of overlapping peaks. PLUTO is running under Microsoft Windows 3.11, 95 and NT.

3. Results and discussion

Organic matter found in cometary dust contains carbon, hydrogen, oxygen, nitrogen, and possibly some sulfur. Reliable data are available only for elemental abundances; however, molecular structure information [5,18,19] is still poor. In the course of this work 60 selected reference compounds have been investigated (see the Appendix); some of them are likely to occur in the organic phase of cometary dust (for instance, unsaturated nitrogen containing compounds); others have been included because of their methodical relevance. From these we chose two substance classes: (1) dicarboxylic acids, very probably not being present in comets, and (2) nucleobases, very probably present in comets, and important for the origin of life. For four of these compounds (Fig. 1) data for positive and negative SIMS, positive and negative PDMS, and electron ionization (EI) spectra [20] are compared in the following.

In general it is known that surface ionization methods based on rapid dissipation of energy produce the same types of ions, however, mostly in different relative abundances. Despite the high energy in SIMS and the extreme high energy in PDMS [21] of the impacting particles the excitation energy of the quasimolecular ions is much lower than with EI; consequently less fragment ions are produced that can be used to derive structural information. The investigated compounds show in SIMS and PDMS quasimolecular

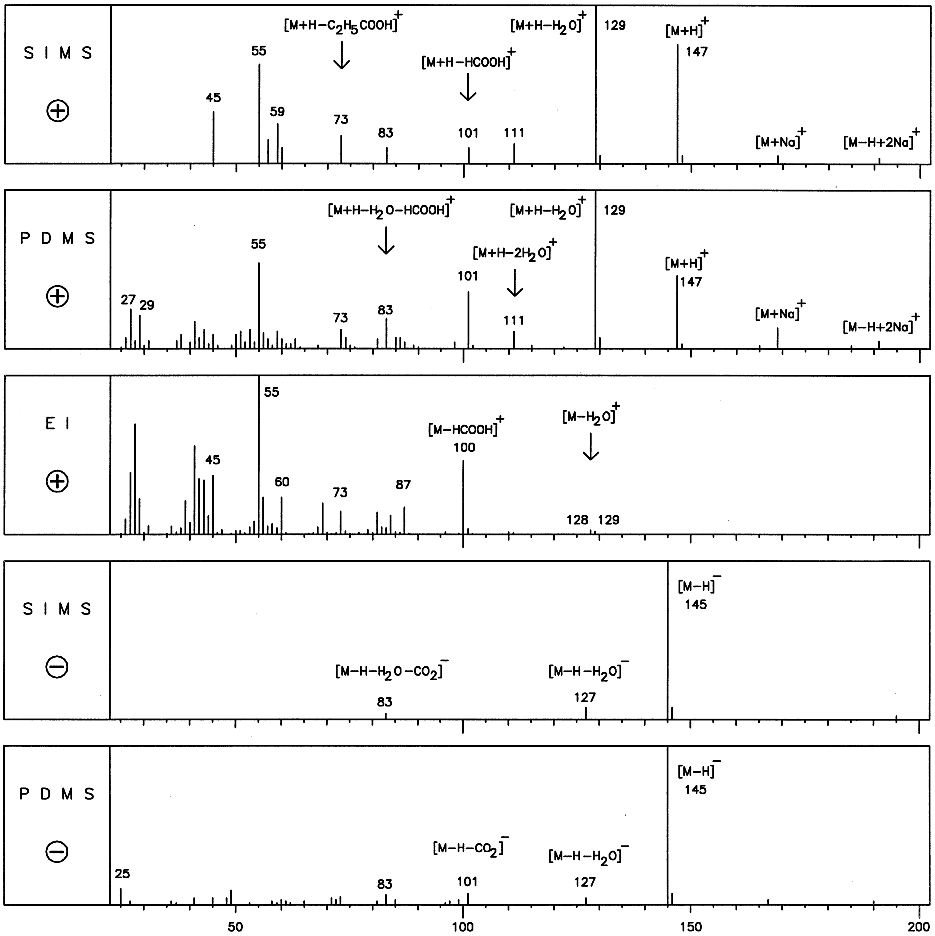

Fig. 2. SIMS, PDMS, and EI data for adipic acid (mw 146).

ions of the type $[M + H]^+$ for the positive and $[M–H]^-$ for the negative mode. Also dimer and trimer formation can be detected in both modes, leading to ions $[2M + H]^+$, $[3M + H]^+$, $[2M–H]^-$, and $[3M–H]^-$. Sodium and in some cases potassium adducts of some of these molecular species can be seen in the positive mode, for instance $[M + Na]^+$, $[2M + Na]^+$, $[M + K]^+$, and $[2M + K]^+$. Ions $[M–H + 2Na]^+$ are also observed in the spectra and may be the quasimolecular ions of sodium salts that are probable contaminants of the acids. Most of the prominent fragment ions are identical in SIMS and PDMS, however, the relative intensities are different. Intensities of neutral loss fragments in SIMS are in general lower than those in PDMS. This effect may be due to the different time windows for the detection of fragment ions (as mentioned in sec. 2). Fragments of the low mass region such as the abundant cyanide ion (*m/z* 26) in the negative spectra of nitrogen containing compounds seem to be often more prominent in SIMS than in PDMS.

3.1. Dicarboxylic acids

Adipic acid and fumaric acid have been selected to demonstrate the principal fragmentation occurring in saturated and unsaturated dicarboxylic acids. Figs. 2 and 3 contain SIMS and PDMS data in positive and in

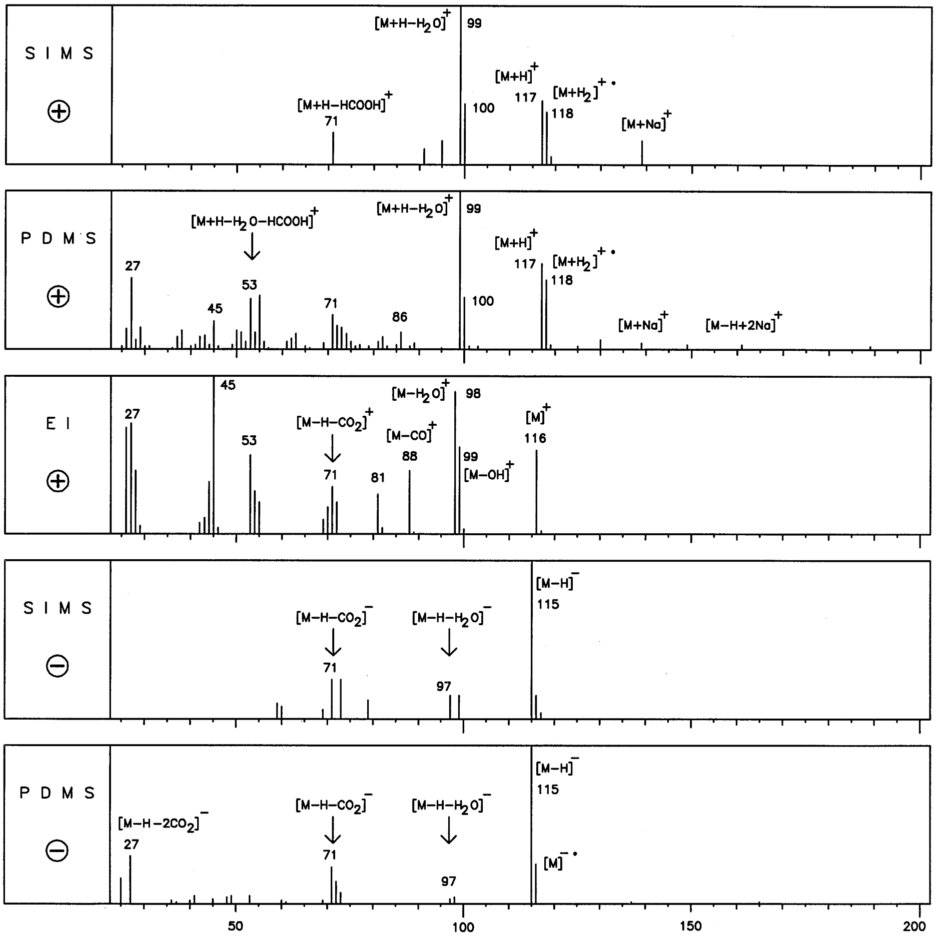

Fig. 3. SIMS, PDMS, and EI data for fumaric acid (mw 116).

negative ion mode and the EI mass spectrum for adipic acid (hexanedioic acid) and fumaric acid (trans-butenedioic acid), respectively. A comparison of common features and differences within the PDMS spectra of these two compounds is shown in Tables 1 and 2.

3.1.1. Positive PDMS and SIMS

Neutral losses of small molecules from the quasi-molecular ion $[M + H]^+$ are the most prominent fragmentations in both compounds. Loss of water $[M + H–H_2O]^+$ gives a strong signal that is often the base peak in the spectra of dicarboxylic acids. Loss of formic acid alone $[M + H–HCOOH]^+$ and combined with the loss of water $[M + H–HCOOH–H_2O]^+$ are also important features of the spectra. Loss of two water molecules is seen only in adipic acid. Common low mass ions at *m/z* 55, $[C_4H_7]^+$ or $[C_3H_3O]^+$, *m/z* 45, $[COOH]^+$ or $[C_2H_5O]^+$, and *m/z* 31, $[CH_3O]^+$, are the same as known from electron ionization mass spectra.

Adipic acid shows a complete modulo-14 ion series with *m/z* 45, 59, 73, 87, and 101, probably corresponding to $[C_nH_{2n-1}O_2]^+$ (*m/z* 45, 59, and 73 may be also $[C_nH_{2n+1}O]^+$; see the discussion of EI spectra). This series does not arise in the spectrum of fumaric acid because of the too short chain length and the unsaturation.

Table 1
PDMS data of adipic acid ($C_6H_{10}O_4$, mw 146)

m/z	Ion	Remarks
		Positive ion mode
147	$[(M + H)]^+$	
129	$[(M + H)–H_2O]^+$	Same neutral loss in fumaric acid
111	$[(M + H)–2H_2O]^+$	
101	$[(M + H)–HCOOH]^+$	Same neutral loss in fumaric acid $[C_nH_{2n-1}O_2]^+$, $n = 5$
87	$[(M + H)–CH_3COOH]^+$	$[C_nH_{2n-1}O_2]^+$, $n = 4$
83	$[(M + H)–H_2O–HCOOH]^+$	
73	$[(M + H)–C_2H_5COOH]^+$	$[C_nH_{2n-1}O_2]^+$, $n = 3$
59	$[(M + H)–C_3H_7COOH]^+$	$[C_nH_{2n-1}O_2]^+$, $n = 2$
55	$[C_4H_7]^+$ or $[C_3H_3O]^+$	Same ion in fumaric acid
45	$[COOH]^+$ or $[C_2H_5O]^+$	Same ion in fumaric acid
31	$[CH_3O]^+$	Same ion in fumaric acid
29	$[C_2H_5]^+$ or $[CHO]^+$	Same ion in fumaric acid
27	$[C_2H_3]^+$	Same ion in fumaric acid
		Negative ion mode
145	$[M–H]^-$	
127	$[(M–H)–H_2O]^-$	Same neutral loss in fumaric acid
101	$[(M–H)–CO_2]^-$	Same neutral loss in fumaric acid
83	$[(M–H)–H_2O–CO_2]^-$	Same neutral loss in fumaric acid
25	$[C_2H]^-$	Same ion in fumaric acid

All prominent ions from adipic acid are nonradical, which is not the case with fumaric acid. Although it is known [22] that a conjugated double bond or an aromatic system can stabilize radicals and this can lead to radical cations $M^{+\cdot}$ identical to electron ionization, a $[M + 2H]^{+\cdot}$ radical cation (*m/z* 118) has not been expected. For this ion and the fragment *m/z* 100 (which is also a radical cation) a fast reaction of the quasimolecular ions in the gas phase is proposed. The carbon–carbon double bond may be attacked by free hot hydrogen radicals (which are highly available under the conditions of SIMS or PDMS excitation) and a water molecule is eliminated (Scheme 1).

3.1.2. Electron impact

The starting point of fragmentation reactions in electron ionization mass spectra is always the molecular radical cation. Therefore, other reaction pathways and mechanisms are possible in comparison with the reactions from nonradical quasimolecular ions. Although the same neutral losses (H_2O and HCOOH) occur from the molecular species, the resulting ions have an odd number of electrons. The McLafferty rearrangement (adipic acid: *m/z* 60) also conserves the radical property. Molecular ions of fumaric acid show losses of CO and CO_2.

The transition from odd electron ions to even electron pathways occurs by α cleavage (adipic acid: *m/z* 45 and 129; fumaric acid: *m/z* 45 and 99) or by inductive cleavage (fumaric acid: *m/z* 71) or by double hydrogen rearrangements such as the γ cleavage (adipic acid: *m/z* 73). The prominent ions *m/z* 55 seem to have a high stability in both electron impact and PDMS, although they must have a different genesis. The sum formula $C_nH_{2n-1}O_2$ for *m/z* 73 and 87 in adipic acid has been confirmed by high mass resolution measurements.

3.1.3. Negative PDMS and SIMS

In contrary to the positive mode the fragment ions exhibit only weak signals in negative spectra. Loss of water from the quasimolecular ion is similar to positive ion spectra; the carboxyl group is eliminated as CO_2; loss of formic acid is not observed. Combined loss of CO_2 and H_2O is only present in the adipic acid

Table 2
PDMS data of fumaric acid ($C_4H_4O_4$, mw 116)

m/z	Ion	Remarks
		Positive ion mode
118	$[M + 2H]^{+\cdot}$	
117	$[(M + H)]^+$	
100	$[(M + 2H)–H_2O]^{+\cdot}$	
99	$[(M + H)–H_2O]^+$	Same neutral loss in adipic acid
86	$[(M + 2H)–CH_3OH]^{+\cdot}$	$[C_3H_2O_3]^{+\cdot}$
71	$[(M + H)–HCOOH]^+$	Same neutral loss in adipic acid
55	$[C_4H_7]^+$ or $[C_3H_3O]^+$	Same ion in adipic acid
53	$[(M + H)–H_2O–HCOOH]^+$	Same neutral loss in adipic acid
45	$[COOH]^+$ or $[C_2H_5O]^+$	Same ion in adipic acid
31	$[CH_3O]^+$	Same ion in adipic acid
29	$[C_2H_5]^+$ or $[CHO]^+$	Same ion in adipic acid
27	$[C_2H_3]^+$	Same ion in adipic acid
		Negative ion mode
116	$[M]^{-\cdot}$	
115	$[M–H]^-$	
98	$[M–H_2O]^{-\cdot}$	
97	$[(M–H)–H_2O]^-$	Same neutral loss in adipic acid
73	$[(M–H)–CH_2CO]^-$	
71	$[(M–H)–CO_2]^-$	Same neutral loss in adipic acid
53	$[(M–H)–H_2O–CO_2]^-$	Same neutral loss in adipic acid
27	$[(M–H)–2CO_2]^-$	$[C_2H_3]^-$
25	$[C_2H]^-$	Same ion in adipic acid

spectrum; in fumaric acid, loss of two CO_2 molecules produces a prominent peak at *m/z* 27.

Formation of the radical anion *m/z* 116 (with fumaric acid) can be explained in analogy to Scheme 1 by a fast reaction in the gas phase. The radical anions *m/z* 98 and 72 are produced by losses of H_2O or CO_2 from these molecular species.

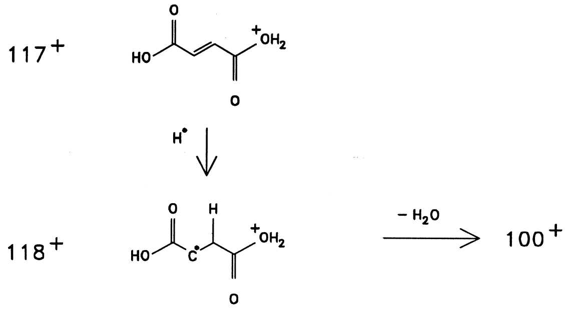

Scheme 1.

3.2. Purine nucleobases

Adenine and guanine have been selected because of interest in the principal fragmentations occurring in purine nucleobases, which are assumed to be present in cometary dust. Nitrogen is the only heteroelement in adenine that formally is a pentamer of HCN and guanine additionally contains oxygen. For both molecules the presence of nitrogen is significantly represented in the spectra; in the spectrum of guanine features characteristic for oxygen are present.

Figs. 4 and 5 contain SIMS and PDMS data in positive and in negative ion mode and the EI mass spectrum for adenine and guanine. A comparison of common features and differences within the PDMS spectra of these two purine nucleobases is shown in Tables 3 and 4.

3.2.1. Positive PDMS and SIMS

Characteristic fragmentations of the protonated molecules $[M + H]^+$ are losses of one or more

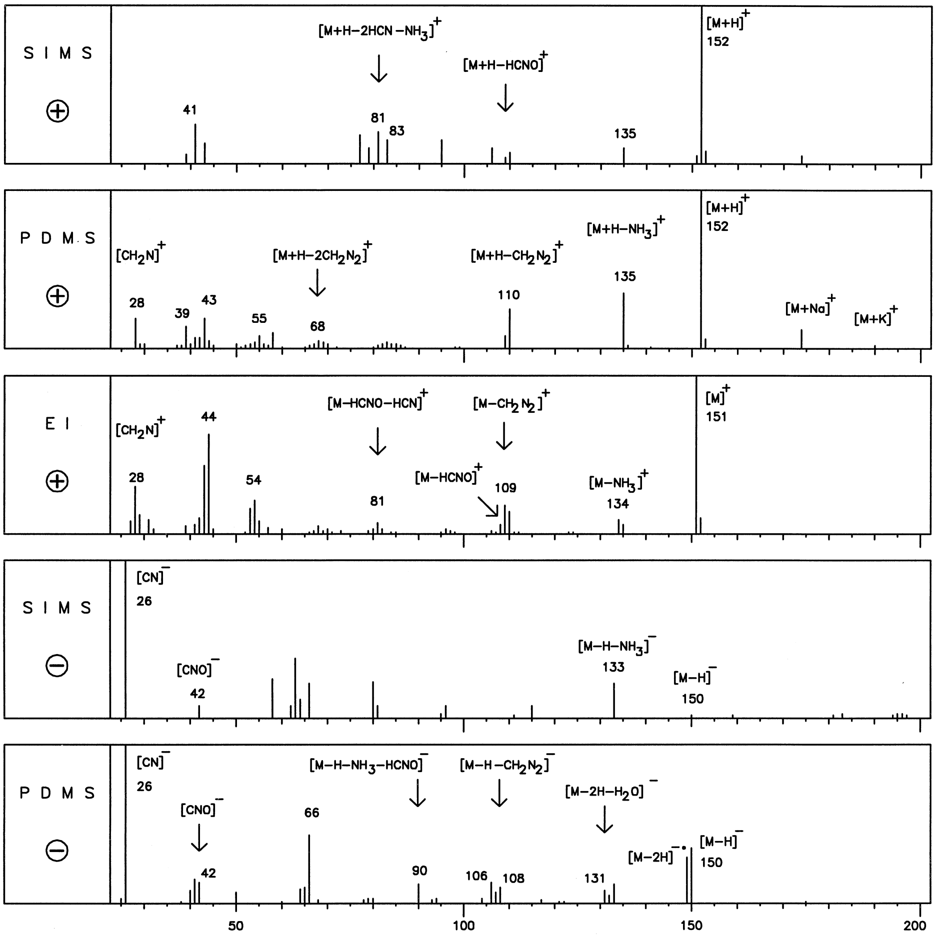

Fig. 5. SIMS, PDMS, and EI data for guanine (mw 151).

nitrogen-containing small molecules, such as NH_3, HCN, or CH_2N_2, in guanine also HCNO; however, the oxygen in guanine does not dominate the neutral loss pattern. An ion series of protonated HCN oligomers (*m/z* 109, 82, 55, 28) is present in adenine and guanine. The smallest ion of this series $[CH_2N]^+$ (*m/z* 28) is the most abundant fragment in the low mass region of the PDMS spectrum. No prominent oxygen-containing low mass ions such as *m/z* 31 or *m/z* 45 arise in the spectrum of guanine. All these fragment ions are nonradical ions, the only exception seems to be *m/z* 133, $[(M + H)–3H]^{+\cdot}$, in the adenine PDMS spectrum.

The ion $[C_3H_3]^+$ is often present in spectra of unsaturated and aromatic compounds. In the SIMS measurements the mass resolution was sufficiently high to distinguish $[C_3H_3]^+$ and $[K]^+$, both at nominal mass *m/z* 39; only the first one is considered in the presented SIMS data.

3.2.2. Electron ionization

Electron ionization spectra of the investigated purine nucleobases differ from SIMS and PDMS data, although similarities in neutral loss chemistry can be detected. Prominent losses in adenine are HCN and CH_2N_2, in guanine also NH_3 and HCNO; all these fragment ions are radical species contrary to those in SIMS and PDMS.

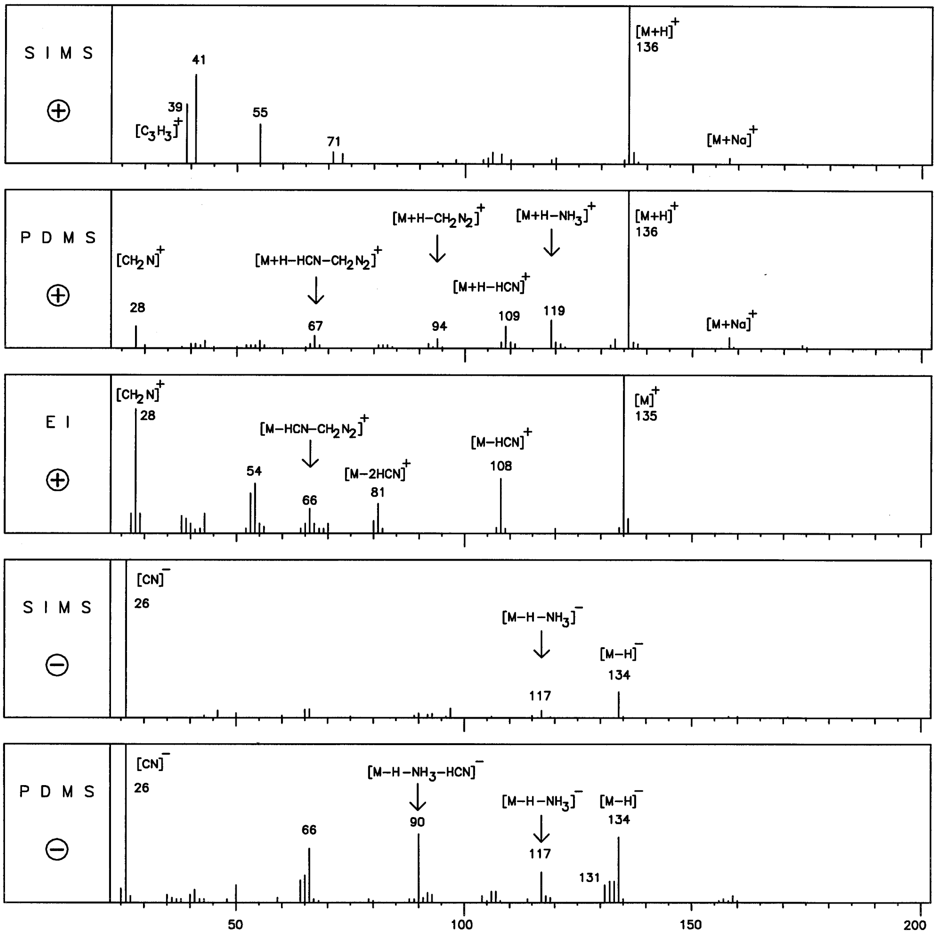

Fig. 4. SIMS, PDMS, and EI data for adenine (mw 135).

The members of the HCN oligomer ion series *m/z* 108, 81, 54, 27 present in the electron ionization spectra of adenine and guanine are also radical ions. The most prominent ion of this series is the dimer at *m/z* 54 accompanied in both spectra by an ion *m/z* 53. The HCN monomer is accompanied by an abundant ion $[CH_2N]^+$ (*m/z* 28) which is the same nonradical species as present in PDMS.

3.2.3. Negative PDMS and SIMS

Losses of NH_3, HCN and CH_2N_2 from the deprotonated molecule $[M–H]^-$ are similar to those in positive spectra. Loss of oxygen containing species is more abundant in the negative PDMS spectra than in the positive counterparts. Note that the loss of H_2O, NH_2OH, or HCNO in guanine corresponds to the loss of H_2, NH_3, or HCN, respectively, in adenine, producing the same ions.

The base peak in SIMS and in PDMS is for both compounds at *m/z* 26 corresponding to $[CN]^-$ ions; this peak is very abundant for all investigated nitrogen-containing organic compounds. The fragment *m/z* 42, $[CNO]^-$, which is present in guanine, often arises from organic species containing both oxygen and nitrogen atoms. Its abundance increases if the substructure N–C═O is present and can even compete with the intensity of $[CN]^-$ for multiple occurrences of this substructure.

Table 3
PDMS data of adenine ($C_5H_5N_5$, mw 135)

m/z	Ion	Remarks
		Positive ion mode
136	$[(M + H)]^+$	
133	$[(M + H)–3H]^{+\cdot}$	$[C_5H_3N_5]^{+\cdot}$
119	$[(M + H)–NH_3]^+$	Same neutral loss in guanine
109	$[(M + H)–HCN]^+$	$[(HCN)_4 + H]^+$, same ion in guanine
94	$[(M + H)–CH_2N_2]^+$	Same neutral loss in guanine
92	$[(M + H)–NH_3–HCN]^+$	
82	$[(HCN)_3 + H]^+$	Same ion in guanine
67	$[(M + H)–HCN–CH_2N_2]^+$	$[C_3H_3N_2]^+$, same neutral loss in guanine, Same ion in guanine
55	$[(HCN)_2 + H]^+$	Same ion in guanine
28	$[(HCN)_1 + H]^+$	Same ion in guanine
		Negative ion mode
134	$[M–H]^-$	
133	$[M–2H]^{-\cdot}$	Same neutral loss in guanine
132	$[(M–H)–H_2]^-$	Same ion in guanine
131	$[(M–2H)–H_2]^{-\cdot}$	$[C_5HN_5]^{-\cdot}$, same ion in guanine
117	$[(M–H)–NH_3]^-$	$[C_5HN_4]^-$, same neutral loss in guanine, Same ion in guanine
107	$[(M–H)–HCN]^-$	$[C_4H_3N_4]^-$, same ion in guanine
106	$[(M–2H)–HCN]^{-\cdot}$	$[C_4H_2N_4]^{-\cdot}$, same ion in guanine
92	$[(M–H)–CH_2N_2]^-$	Same neutral loss in guanine
90	$[(M–H)–NH_3–HCN]^-$	$[C_4N_3]^-$, same neutral loss in guanine, Same ion in guanine
66	$[C_4H_4N]^-$ or $[C_2N_3]^-$,	Same ion in guanine
26	$[CN]^-$	Same ion in guanine

The PDMS spectra of both compounds contain a prominent peak at *m/z* 90 corresponding to $[C_4N_3]^-$; this ion can be produced from adenine by the combined loss of NH_3 and HCN, and from guanine by the combined loss of NH_3 and HCNO. The pyrimidine ring (respectively, tautomeric analogues) with at least one nitrogen atom on one of the carbon atoms seems to be the characteristic substructure responsible for this fragment. This suggestion has risen from a systematic comparison of the molecular structures of relevant compounds. A group of 12 compounds (from the 60 measured compounds) showing a significant abundance of ions *m/z* 90 has been searched for large and frequently occurring substructures. For each of the possible 78 pairs of these 12 structures the maximum common substructure [23,24] has been determined. The size of a substructure has been measured by the number of nonhydrogen atoms; all bond types have been treated as being equivalent. The 78 maximum common substructures found have been ranked by the number of occurrences in the 12 molecular structures. The first three hits (after eliminating duplicates) are shown in Fig. 6. This result gives evidence for a N-substituted pyrimidine ring being responsible for peak *m/z* 90; actually such a substructure is contained in all 12 compounds which exhibit a prominent peak at this mass number. The above described exploration of chemical structures has been performed by software ToSiM [25].

The peak group *m/z* 66, 65, and 64 is prominent in the PDMS spectra from adenine and guanine; possible formulas for *m/z* 66 (always the highest peak in this group) are $[C_2N_3]^-$ and $[C_4H_4N]^-$; the latter is a nitrogen containing analogon to the aromatic fragment $[C_5H_5]^-$ (see the Appendix). From 20 measured compounds containing a pyrimidine ring or a structure tautomeric to it 18 exhibit a characteristic peak pattern *m/z* 66, 65, and 64 in their negative PDMS spectra.

Table 4
PDMS data of guanine ($C_5H_5N_5O$, mw 151)

m/z	Ion	Remarks
		Positive ion mode
152	$[(M + H)]^+$	
135	$[(M + H)–NH_3]^+$	Same neutral loss in adenine
110	$[(M + H)–CH_2N_2]^+$	Same neutral loss in adenine
109	$[(M + H)–HCNO]^+$	$[(HCN)_4 + H]^+$, same ion in adenine
83	$[(M + H)–HCN–CH_2N_2]^+$	Same neutral loss in adenine
82	$[(HCN)_3 + H]^+$	Same ion in adenine
68	$[(M + H)–2CH_2N_2]^+$	
67	$[(M + H)–HCNO–CH_2N_2]^+$	$[C_3H_3N_2]^+$, same ion in adenine
55	$[(HCN)_2 + H]^+$	Same ion in adenine
28	$[(HCN)_1 + H]^+$	Same ion in adenine
		Negative ion mode
150	$[M–H]^-$	
149	$[M–2H]^{-\cdot}$	Same neutral loss in adenine
133	$[(M–H)–NH_3]^-$	
132	$[(M–H)–H_2O]^-$	Same ion in adenine
131	$[(M–2H)–H_2O]^{-\cdot}$	$[C_5HN_5]^{-\cdot}$, same ion in adenine
117	$[(M–H)–NH_2OH]^-$	$[C_5HN_4]^-$, same ion in adenine
108	$[(M–H)–CH_2N_2]^-$	Same neutral loss in adenine
107	$[(M–H)–HCNO]^-$	$[C_4H_3N_4]^-$, same ion in adenine
106	$[(M–2H)–HCNO]^{-\cdot}$	$[C_4H_2N_4]^{-\cdot}$, same ion in adenine;
	$[(M–H)–NH_3–HCN]^-$	$[C_4N_3O]^-$, same neutral loss in adenine
90	$[(M–H)–NH_3–HCNO]^-$	$[C_4N_3]^-$, same ion in adenine
66	$[C_4H_4N]^-$ or $[C_2N_3]^-$,	Same ion in adenine
42	$[CNO]^-$	
26	$[CN]^-$	Same ion in adenine

The PDMS data from guanine show a surprisingly strong $[M–2H]^{-\cdot}$ radical anion at *m/z* 149; the corresponding ion *m/z* 133 in the adenine spectrum has much lower abundance. From this ion species H_2 and HCN are lost in adenine, whereas H_2O and HCNO are lost in guanine; from both compounds the same radical ions at *m/z* 131 and 106 are produced by these fragmentations. Note that *m/z* 106 in guanine may also correspond to $[M–H–NH_3–HCN]^-$.

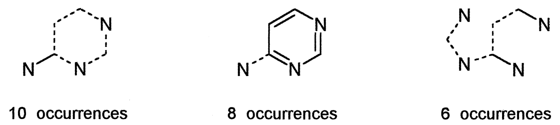

Fig. 6. Characteristic substructures for 12 compounds exhibiting a significant peak at *m/z* 90, probably $[C_4N_3]^-$, in negative ion PDMS spectra. Dashed lines denote bonds of any type.

4. Conclusions

From the examples discussed and from other experimental results it follows that SIMS and PDMS data are, in general, very similar, although the ionization processes and the time scales for the detection of fragment ions are different. Most ions in SIMS and PDMS are nonradical; that means the even-electron quasimolecular ions decay, if at all, by the elimination of small stable molecules. Exceptions exist for unsaturated and aromatic species where radical ion formation is possible and decay products can be stabilized.

Chemometric methods for modeling relationships between spectral data and structural properties require the definition of a set of appropriate variables (spectral features). These features should reflect structural information and have to be determined automatically from the mass spectral peak list. To support the creation of efficient spectral features the typical ion fragmentation processes occurring in SIMS and PDMS have been summarized by a set of rules in the Appendix.

The peculiarities of ion formation and fragmentation processes in SIMS and PDMS will require a transformation of the spectral data, which is in some parts different to the transformation used for EI spectra [16,26]. Three conclusions can be drawn. (1) Because eliminations of small molecules are most prominent it is promising to create spectral features that characterize certain mass differences. (2) The presence of a series of key ions in a spectrum may be characteristic for the presence of a particular substructure. For instance, the joint presence of a prominent peak at *m/z* 90 and a group of peaks at *m/z* 66, 65, and 64 (dominated by *m/z* 66) is a hint for a pyrimidine substructure substituted by at least one additional nitrogen atom. Purine nucleobases or related compounds—which are supposed to be present in comet dust—belong to this compound class. (3) Fragment ions exist in the low mass range of positive and negative spectra characterizing compound classes and heteroatom content.

Preliminary results [27] of modeling relationships between PDMS data and some simple structural properties (for instance, the content of nitrogen in percent of the molecular mass) indicate that features based on spectroscopic knowledge are better suited than features defined solely by mathematical concepts. The comparison of SIMS and PDMS data indicates that PDMS data are suitable for testing chemometric methods relevant to automatic data evaluation in the COSIMA experiment.

Acknowledgements

The authors thank E. Jessberger (Institute of Planetology, University of Münster, Germany) for making possible the SIMS experiments, and S.E. Stein (NIST, Gaithersburg, MD, USA) for providing the NIST Mass Spectral Database. Collaborations of H. Botay, B. Stanschitz (PDMS measurements), and W. Demuth (software development) are greatly acknowledged. This work was supported in Austria by Österreichische Akademie der Wissenschaften, project no. 6070/16-III/A/5/98, and in Germany by Deutsche Agentur für Raumfahrtangelegenheiten (DARA), project no. FKZ 50 QP 9711.

Appendix: Rules for ion formation and fragmentation in SIMS and PDMS

1. Quasimolecular ions

Radical molecular ions are not formed, except from polycyclic aromatic hydrocarbons (PAH) and some unsaturated compounds that may, under radical attack, form mesomerically stabilized radicals. Especially with N- and/or P-bearing (basic) molecules $[M + H]^+$ ions are preferably produced; $[M–H]^-$ is less often abundant. With O- and/or S-bearing (acidic) molecules $[M–H]^-$ is preferably produced and $[M + H]^+$ is less abundant. In most cases the proton affinity of those sites determines the relative abundances of positive and negative quasimolecular ions. Molecules for which cationization is possible often form $[M + \text{metal}]^+$ ions if Cu, Ag, or Au is used for the target in SIMS; to a lesser extent, ions $[2M + \text{metal}]^+$ and $[3M + \text{metal}]^+$ or, even $[3M + 2\text{metal}–H]^+$, are produced. Ia- and Ib-metal adducts are rather stable ions which only undergo minor elimination reactions (for instance elimination of water). Negative quasimolecular ions in general fragment to a lesser extent than positive ones.

Polar molecules show in the presence of traces of alkali salts the adduction of alkali cations (group Ia elements) leading to ions $[M + \text{alkali}]^+$, but also ions $[M + 2Na–H]^+$ or $[M + 3Na–2H]^+$ may be formed. Halogen anion adduction leading to $[M + \text{halogen}]^-$ is restricted to some polar halogenated species, and cannot be induced by just adding halide salts.

Cationic salts (for instance tetraalkylammonium) produce intensive nonradical cations (for instance $[(CH_3)_4N]^+$); anionic salts (for instance, some tensides) produce nonradical anions.

Comparing with EI the radical ions in SIMS and PDMS are suppressed by (1) more than two orders of magnitude for ionic species present as organic salts; (2) one to two orders of magnitude for polar, but nonionic species; (3) less than one order of magnitude for hydrocarbons; and (4) no suppression occurs for PAH's and some other unsaturated species with which radicals are well stabilized.

The total ion formation in SIMS and PDMS increases with increasing polarity of the molecules; this especially holds for positive ions from N-containing molecules and for negative ions from O- or S-containing molecules.

2. Elimination reactions

Elimination of small molecules, especially H_2, H_2O, C_nH_{2n}, HCOOH, HCHO, CO, NH_3, HCN, and H_2S is the most prominent fragmentation process of positive and negative quasimolecular ions.

A water molecule is eliminated from alcohols, polyalcohols (sugars), carboxylic acids (but not from their esters), ketones, and ethers; if possible two or even three water molecules may be released. Adduct ions containing a cation of a Ia or Ib element almost only decay by water elimination.

Formic acid elimination is important for carboxylic acids (not for their esters) and is heavily enhanced by polar sites in α position (for instance, in natural amino acids). Carbon monoxide elimination is found with aromatic or alicyclic oxygen compounds.

Elimination of ammonia and hydrogencyanide occurs frequently in N-heterocyclic compounds.

3. Characteristic small fragment ions

Hydrocarbons: $[CH]^+$, $[CH]^-$, $[C_2H]^-$, $[C_2H_3]^+$; alkenes and cycloalkanes: $[C_nH_{2n-1}]^+$; aromatic compounds: $[C_3H_3]^+$, $[C_5H_5]^-$, $[C_7H_7]^+$; N-containing compounds: $[NH_2]^-$, $[NH_4]^+$, $[CN]^-$, $[CH_2N]^+$; O-containing compounds: $[OH]^-$, $[H_3O]^+$, $[CHO]^-$, $[CH_3O]^+$; N- and O-containing compounds: $[CNO]^-$, $[CH_2NO]^+$; phenylalkyl compounds: $[C_6H_5]^+$, $[C_7H_7]^+$, $[C_8H_9]^+$; some amines (alkenyl, cycloalkyl, or cyclic): $[C_nH_{2n}N]^+$.

References

[1] A.E. Ashcroft, Ionization Methods in Mass Spectrometry, The Royal Society of Chemistry, Cambridge, 1997.
[2] International ROSETTA Mission by the European Space Agency. Launch is planned for year 2003; rendevouz with comet 46p/Wirtanen is expected in year 2011. A part of the spacecraft will land on the comet; the COSIMA experiment will take place in an orbit around the comet.
[3] Comet 46p/Wirtanen. Discovered in 1948 by C.A. Wirtanen, Lick Observatory, California. The character "p" denotes a periodic comet. Orbital period 6.7 years; perihelion distance (nearest distance to sun) 1.1 a.u.; a close approach to earth happened in March 1997 at a distance of 1.5 a.u. (1 a.u. = 1.5×10^8 km).
[4] COSIMA (Cometary Secondary Ion Mass Analyzer) will be one of the instruments aboard the ROSETTA spacecraft. Principal investigator is one of the authors (J.K.).
[5] J. Kissel, F.R. Krueger, Nature 326 (1987) 755.
[6] J. Kissel, D.E. Brownlee, K. Büchler, B.C. Clark, H. Fechtig, E. Grün, K. Hornung, E.B. Igenbergs, E.K. Jessberger, F.R. Krueger, H. Kuczera, J.A.M. McDonnell, G.M. Morfill, J. Rahe, G.H. Schwehm, Z. Sekanina, N.G. Utterback, H.J. Völk, H.A. Zook, Nature 321 (1986) 336.
[7] J. Kissel, R.Z. Sagdeev, J.L. Bertaux, V.N. Angarov, J. Audouze, J.E. Blamont, K. Büchler, E.N. Evlanov, H. Fechtig, M.N. Fomenkova, H. von Hoerner, N.A. Inogamov, V.N. Khromov, W. Knabe, F.R. Krueger, Y. Langevin, V.B. Leonas, A.C. Levasseur-Regourd, G.G. Managadze, S.N. Podkolzin, V.D. Shapiro, S.R. Tabaldyev, B.V. Zubkov, Nature 321 (1986) 280.
[8] J.M. Greenberg, Astron. Astrophys. 330 (1998) 380.
[9] J.P. Bradley, Science 265 (1994) 925.
[10] N.G. Utterback, J. Kissel, Astrophys. J. 100 (1990) 1315.
[11] F.R. Krueger, J. Kissel, Origins Life Evolution Biosphere 19 (1989) 87.
[12] K. Varmuza, W. Werther, J. Chem. Inf. Comput. Sci. 36 (1996) 323.
[13] W. Werther, K. Varmuza, in Software-Development in Chemistry, C. Jochum (Ed.), Gesellschaft Deutscher Chemiker, Frankfurt am Main, 1994, Vol. 8, p. 129.
[14] M. Guilhaus, J. Mass Spectrom. 30 (1995) 1519.
[15] K. Varmuza, W. Demuth, W. Werther, E.R. Schmid, F.R. Krueger, unpublished.
[16] W. Demuth, diploma work, Vienna University of Technology, Faculty of Sciences, 1998.
[17] R.S. Juvet, G.M. Allmaier, E.R. Schmid, Anal. Chim. Acta 241 (1990) 241.
[18] M.E. Lawler, D.E. Brownlee, Nature 359 (1992) 810.
[19] C. Joblin, C. Masselon, P. Boissel, P. de Parseval, S. Martinovic, J.F. Muller, Rapid Commun. Mass Spectrom. 11 (1997) 1619.
[20] NIST Mass Spectral Database, version 4, National Institute of Standards and Technology, Gaithersburg, MD, 1992.
[21] B. Sundqvist, R.D. Macfarlane, Mass Spectrom. Rev. 4 (1985) 421.

[22] S. Bourcier, Y. Hoppilliard, T. Kargar, Rapid Commun. Mass Spectrom. 11 (1997) 1046.
[23] H. Scsibrany, K. Varmuza, Fresenius J. Anal. Chem. 344 (1992) 220.
[24] K. Varmuza, P.N. Penchev, H. Scsibrany, J. Chem. Inf. Comput. Sci. 38 (1998) 420.
[25] H. Scsibrany, K. Varmuza, Software ToSiM (Topological Similarities of Molecules), MS-DOS program; available from author K.V.
[26] K. Varmuza, W. Werther, in Advances in Mass Spectrometry, E.J. Karjalainen, A.E. Hesso, J.E. Jalonen, U.P. Karjalainen (Eds.), Elsevier, Amsterdam, 1998, Vol. 14, p. 611.
[27] K. Varmuza, W. Werther, E.R. Schmid, F.R. Krueger, unpublished results.